Featured in Physics

Enhanced Production of Λ_b^0 Baryons in High-Multiplicity pp Collisions at $\sqrt{s} = 13$ TeV

R. Aaij *et al.*[*]
(LHCb Collaboration)

(Received 19 October 2023; revised 19 December 2023; accepted 9 January 2024; published 20 February 2024)

The production rate of Λ_b^0 baryons relative to B^0 mesons in pp collisions at a center-of-mass energy $\sqrt{s} = 13$ TeV is measured by the LHCb experiment. The ratio of Λ_b^0 to B^0 production cross sections shows a significant dependence on both the transverse momentum and the measured charged-particle multiplicity. At low multiplicity, the ratio measured at LHCb is consistent with the value measured in e^+e^- collisions, and increases by a factor of ~2 with increasing multiplicity. At relatively low transverse momentum, the ratio of Λ_b^0 to B^0 cross sections is higher than what is measured in e^+e^- collisions, but converges with the e^+e^- ratio as the momentum increases. These results imply that the evolution of heavy b quarks into final-state hadrons is influenced by the density of the hadronic environment produced in the collision. Comparisons with several models and implications for the mechanisms enforcing quark confinement are discussed.

DOI: 10.1103/PhysRevLett.132.081901

One of the defining features of quantum chromodynamics (QCD) is color confinement, which prohibits isolated quarks and gluons from being observed. Instead, the partons, which carry color charge, are found only as constituents of color-neutral hadrons [1]. Quarks that are produced at colliders such as the Large Hadron Collider (LHC), evolve into observable hadrons through a process known as hadronization. Factorization theorems in QCD typically assume that hadronization is a universal process, independent of the colliding beam species [2].

One mechanism of hadronization is parton-to-hadron fragmentation, where the potential between outgoing partons grows until it is energetically favorable to produce other partons from the vacuum that neutralize the initiating parton's color charge. This process is often modeled by cluster formation [3] or color string breaking [4]. The resulting collections of particles are known as jets [5], and have been studied extensively in e^+e^-, pp, $p\bar{p}$, and heavy-ion collisions [6–13]. Fragmentation functions, which describe the evolution of quarks and gluons resulting from hard scattering into hadrons, are constrained by data from e^+e^- collisions [14–16].

An alternative hadronization mechanism can arise when quarks that are produced near each other combine to form color-neutral hadrons through a process called coalescence. Models of coalescence generally require individual parton wave functions to overlap in position and velocity space, and have successfully described a range of collider and fixed-target data [17–21]. In these models, the density of partons produced in the underlying event has a significant effect on the hadronization process, and is expected to be especially important in heavy-ion collisions [20,22]. Enhanced baryon production can be a signature of coalescence, and models generally require coalescence in order to reproduce the baryon to meson production cross-section ratios measured in heavy-ion collisions [23–25]. Multiple parton interactions in pp collisions can also result in many overlapping color strings and high final-state particle multiplicities. This alternative hadronization mechanism does not require fragmentation, and since charged-particle multiplicity in the underlying event depends on the colliding beam species, the emergence of coalescence in hadron collisions breaks the universality of the hadronization process.

The family of hadrons containing bottom quarks is particularly sensitive to hadronization. Because of the large mass of b quarks, light quark to b-hadron fragmentation is suppressed, and the long wavelengths of heavy b quarks at low transverse momentum p_{T} can potentially overlap with other particles produced in the event. Additionally, there is no b-quark content in the valence quarks of beam particles, and b-quark production is dominated by hard parton-parton interactions in the early stages of the collision, before hadronization takes place [26]. Total $b\bar{b}$ cross sections are consequently well described by perturbative QCD calculations [27–29]. Previous measurements have shown that the fraction of b quarks that hadronize into baryons has a

[*]Full author list given at the end of the Letter.

significant p_T dependence [30,31], and that there is an asymmetry between Λ_b^0 and $\bar{\Lambda}_b^0$ production at the LHC [32]. There is also evidence for an increase in the rate of B_s^0 meson production relative to B^0 production with increasing multiplicity at low p_T [33]. Additionally, the ALICE Collaboration has shown that the fragmentation fractions for charm quarks vary between e^+e^- and pp collisions, with pp data favoring higher Λ_c^+ baryon production [34], and that the baryon production is affected by the multiplicity of the underlying event [35]. None of these results are expected in a scenario where heavy quarks hadronize only via fragmentation in the vacuum. If coalescence is affecting b-quark hadronization, enhanced production of low-p_T Λ_b^0 baryons would be expected in collisions with relatively high multiplicity. In contrast, b quarks produced in low multiplicity collisions and/or at high p_T would have little interaction with other produced particles and fragment in the vacuum, as in e^+e^- collisions.

This Letter presents new measurements of the ratio of Λ_b^0 baryon to B^0 meson production cross sections, as a function of p_T and multiplicity, using a sample of pp collisions at $\sqrt{s} = 13$ TeV corresponding to an integrated luminosity of about 5.4 fb^{-1}. Candidates for Λ_b^0 baryons and B^0 mesons are reconstructed through their decays to the $J/\psi pK^-$ and $J/\psi\pi^-K^+$ final states, respectively (charge conjugation is assumed throughout this Letter), where the J/ψ meson subsequently decays to the $\mu^+\mu^-$ final state.

The LHCb detector [36,37] is a single-arm forward spectrometer covering the pseudorapidity range $2 < \eta < 5$, designed for the study of particles containing b or c quarks. The detector includes a high-precision tracking system consisting of a silicon-strip vertex detector surrounding the pp interaction region [38] (known as the VELO detector), a large-area silicon-strip detector located upstream of a dipole magnet with a bending power of about 4 Tm, and three stations of silicon-strip detectors and straw drift tubes [39] placed downstream of the magnet. The tracking system provides a measurement of the momentum of charged particles with a relative uncertainty that varies from 0.5% at low momentum to 1.0% at 200 GeV/c. Different types of charged hadrons are distinguished using information from two ring-imaging Cherenkov detectors [40]. Muons are identified by a system composed of alternating layers of iron and multiwire proportional chambers [41].

Simulation is required to model the effects of the detector acceptance and the imposed selection requirements. In the simulation, pp collisions are generated using PYTHIA [42]. Decays of unstable particles are described by EVTGEN [43], in which final-state radiation is generated using PHOTOS [44]. The interaction of the generated particles with the detector, and its response, are implemented using the GEANT4 toolkit [45] as described in Ref. [46]. Weights are applied to the simulation to ensure the invariant mass distributions of product pairs from the Λ_b^0 and B^0 decays and the parent p_T match background-subtracted distributions that are extracted from the data using the *sPlot* method [47].

Events considered here are identified by a series of hardware and software triggers designed to select muons from the decay $J/\psi \to \mu^+\mu^-$, and have exactly one reconstructed primary vertex. Each individual muon candidate is required to have $p_T > 500$ MeV/c and to penetrate hadron absorbers in the LHCb muon system. The reconstructed $\mu^+\mu^-$ pair must have a mass within 39 MeV/c^2 of the known J/ψ mass (which corresponds to 3 times the measured mass resolution of the J/ψ peak) [48], and must form an origin vertex that is displaced from the primary vertex. Charged pion, kaon, and proton candidates are positively identified by the response of the LHCb ring-imaging Cherenkov detectors, and are required to have a momentum above 3 GeV/c and $p_T > 750$ MeV/c. Combinations of tracks that meet these requirements are refit with kinematic constraints that fix the $\mu^+\mu^-$ invariant mass to the known J/ψ mass, and require all four tracks to share a common vertex.

The multiplicity metrics used are either the total number of charged tracks reconstructed in the VELO detector, $N_{\text{tracks}}^{\text{VELO}}$, or the subset of backwards VELO tracks that point away from the LHCb spectrometer, $N_{\text{tracks}}^{\text{back}}$, which covers the pseudorapidity interval of approximately $-3.5 < \eta < -1.5$. The backwards VELO tracks provide a multiplicity estimate that is measured in a different rapidity region than the signal. Events containing signal candidates are characterized in terms of their relation to events that are selected by triggering on the LHC beam clock alone, no bias (NB) events, which provide a selection of pp collisions that do not have biases resulting from trigger decisions based on measured particles. The results are quoted in terms of normalized multiplicity, defined as the number of tracks at the center of a given multiplicity bin divided by the mean number of tracks in NB events, which are $\langle N_{\text{tracks}}^{\text{VELO}}\rangle_{\text{NB}} = 37.7$ and $\langle N_{\text{tracks}}^{\text{back}}\rangle_{\text{NB}} = 11.1$, with negligible statistical uncertainties of less than 0.1% [33].

Extended maximum-likelihood fits are performed on the binned $J/\psi pK^-$ and $J/\psi\pi^-K^+$ invariant mass spectra to determine the Λ_b^0 and B^0 yields, respectively, in intervals of p_T and multiplicity. The Λ_b^0 and B^0 signals are each described by a sum of two Crystal Ball functions [49], whose tail parameters and relative contributions are fixed to values determined by fitting simulated decays. The background contribution is represented by an exponential function, which provides a good description of the mass sidebands. Examples of the $J/\psi pK^-$ and $J/\psi\pi^-K^+$ invariant mass distributions and fits are shown in Fig. 1. Variations of the fit functions that converge change the extracted Λ_b^0 and B^0 yields by about 1%, which is taken as a systematic uncertainty.

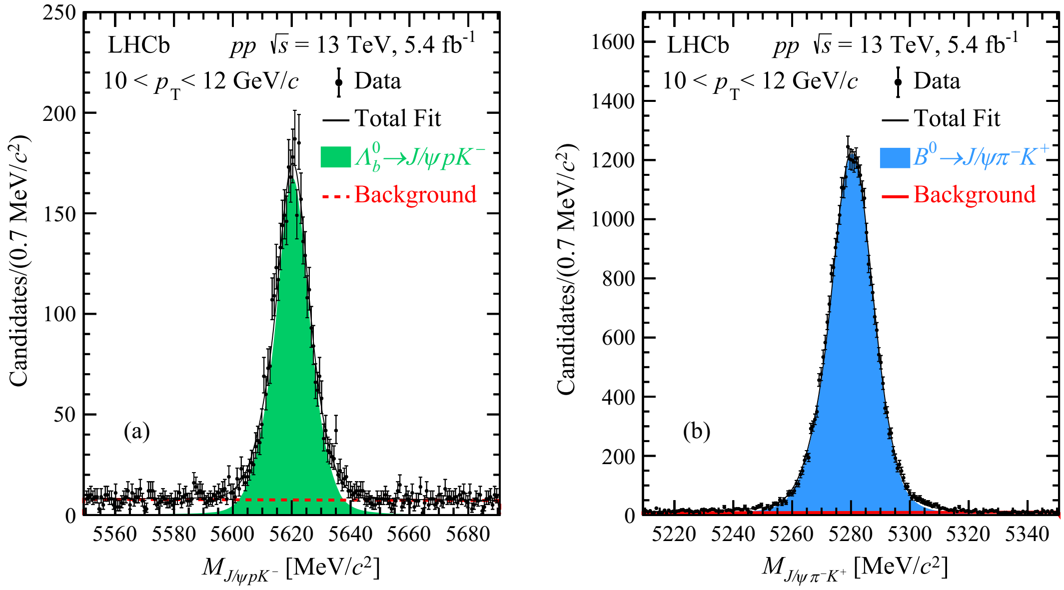

FIG. 1. Invariant mass spectra in the transverse momentum interval $10 < p_T < 12$ GeV/c for the (a) $J/\psi pK^-$ and (b) $J/\psi \pi^- K^+$ final states, integrated over multiplicity. Fit projections including signal and background components are shown.

The ratio of production cross sections $\sigma_{\Lambda_b^0}/\sigma_{B^0}$ is found by calculating

$$\frac{\sigma_{\Lambda_b^0}}{\sigma_{B^0}} = \frac{N_{\Lambda_b^0}}{N_{B^0}} \times \frac{\mathcal{B}_{B^0}}{\mathcal{B}_{\Lambda_b^0}} \times \frac{\epsilon^{\rm acc}_{B^0}}{\epsilon^{\rm acc}_{\Lambda_b^0}} \times \frac{\epsilon^{\rm trig}_{B^0}}{\epsilon^{\rm trig}_{\Lambda_b^0}} \times \frac{\epsilon^{\rm rec}_{B^0}}{\epsilon^{\rm rec}_{\Lambda_b^0}} \times \frac{\epsilon^{\rm PID}_{B^0}}{\epsilon^{\rm PID}_{\Lambda_b^0}}, \qquad (1)$$

where $N_{\Lambda_b^0}$ and N_{B^0} are the Λ_b^0 and B^0 yields extracted by fitting the peaks in the invariant mass spectra, $\mathcal{B}_{\Lambda_b^0}$ and $\mathcal{B}_{B^0}$ are the branching fractions of Λ_b^0 and B^0 to the relevant final states [48], $\epsilon^{\rm acc}$ is the acceptance of the LHCb spectrometer for the given decay, $\epsilon^{\rm trig}$ is the efficiency for triggering on the given decay, $\epsilon^{\rm rec}$ is the efficiency for selecting and reconstructing the parent particle, and $\epsilon^{\rm PID}$ is the total particle identification efficiency for the final-state charged tracks from the decays.

The ratio leads to the partial cancellation of many of the correction factors and their systematic uncertainties due to the similarities of the decays. The ratio of acceptance corrections $\epsilon^{\rm acc}_{B^0}/\epsilon^{\rm acc}_{\Lambda_b^0}$ is estimated via simulation to be ~0.95 at low p_T and tends to unity with increasing p_T. A systematic uncertainty of 1% is evaluated by varying the weights applied to the simulated events within their uncertainties. The ratio of trigger efficiencies $\epsilon^{\rm trig}_{B^0}/\epsilon^{\rm trig}_{\Lambda_b^0}$ is measured as described in Ref. [50], and found to be consistent with unity. Uncertainties on this factor vary from 1% at low p_T to 3% at high p_T, due to the finite size of the data samples used to measure the trigger efficiencies. The ratio of reconstruction efficiencies $\epsilon^{\rm rec}_{B^0}/\epsilon^{\rm rec}_{\Lambda_b^0}$ varies from ~0.8 at the lowest p_T values and increases to be consistent with unity where p_T is much greater than the Λ_b^0 and B^0 masses. The deviation from unity is due to the differences in the reconstruction efficiencies of the intermediate states in the products of the Λ_b^0 and B^0 decays [51–53]. A systematic uncertainty that varies with p_T from 2% to 4% is assigned to account for uncertainties on the weights applied to the simulation, and an additional uncertainty that is negligible at low p_T and increases to a maximum of ~2% at high p_T is assigned to account for the finite size of the simulation samples used to calculate this correction. The ratio of particle identification efficiencies $\epsilon^{\rm PID}_{B^0}/\epsilon^{\rm PID}_{\Lambda_b^0}$ is found using calibrated samples of identified particles taken from data. This term deviates from unity by a maximum of 7% at low p_T, due to the difference in identification efficiencies for pions from B^0 decays and protons from Λ_b^0 decays. A systematic uncertainty of 2% is assigned due to the finite size of the calibration samples [54]. The product of the efficiency ratios ranges from ~0.8 at low p_T to ~0.9 at high p_T. The systematic uncertainty on these corrections is calculated by adding all contributions in quadrature, and ranges between 4% and 6%. Systematic uncertainties dominate for $p_T < 18$ GeV/c, with statistical uncertainties becoming dominant at higher p_T.

The resulting $\sigma_{\Lambda_b^0}/\sigma_{B^0}$ ratio is shown in Fig. 2 as a function of p_T. Numerical values are given in the Supplemental Material [55]. The blue points show the data analyzed in this Letter, where the error bars are the quadrature sum of the statistical and systematic uncertainties, and the error boxes indicate the point-to-point fully correlated (global) uncertainty due to uncertainties on the Λ_b^0 and B^0 branching fractions. The gray points show a previous measurement of the ratio of the Λ_b^0 cross section to the sum of the B^0 and B^+ cross sections measured using

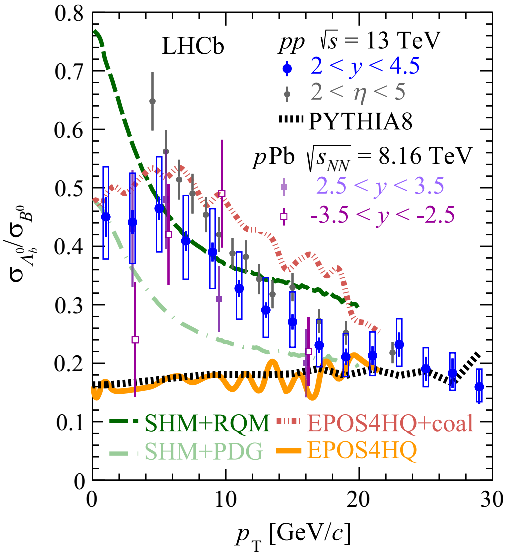

FIG. 2. Ratio of Λ_b^0 to B^0 production cross-sections as a function of p_{T} (blue circles). The error bars represent the quadrature sum of the statistical and systematic uncertainties and the boxes depict the global uncertainties due to branching fractions. The data are compared to previous pp measurements using semileptonic decays (gray circles) [31], and data from pPb collisions (squares) [57]. Calculations from a statistical hadronization model (SHM) [58], and the PYTHIA8 [42] and EPOS4HQ [59] event generators are also shown.

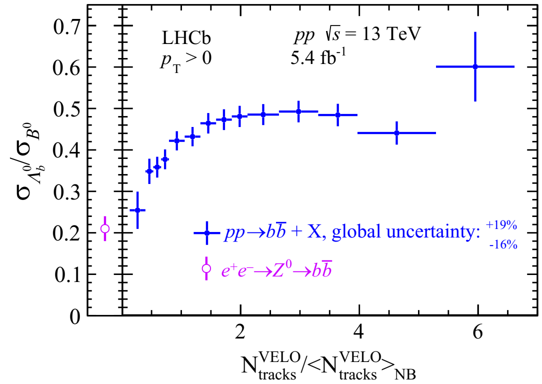

FIG. 3. Ratio of Λ_b^0 to B^0 cross-sections as a function of the total track multiplicity measured in the VELO detector (blue). The purple point indicates the value measured in e^+e^- collisions at LEP [61].

semileptonic decays over the pseudorapidity interval $2 < \eta < 5$ [31]. For direct comparison here, that ratio is multiplied by a factor of 2 under the assumption of equal production of B^0 and B^+ mesons, which is supported by data [56]. In the p_{T} range where the measurements overlap, there is good agreement within uncertainties. Data from pPb collisions [57] covering two different rapidity intervals are also shown for comparison (purple points), and generally agree with the pp data within uncertainties.

The solid green and dashed dark green curves in Fig. 2 are from a recent model of statistical hadronization of b quarks [58] that assumes relative chemical equilibrium between different b-hadron yields, and considers two sets of b hadrons as input. The green solid curve uses the measured spectrum of baryons collected by the Particle Data Group (PDG) in Ref. [48], while the dark dashed curve uses an expanded set of b baryons that are expected by the relativistic quark model (RQM) [60]. Feed-down contributions from these baryons would contribute to the Λ_b^0 yields. The central values of the data are most consistent the RQM calculation at intermediate p_{T}, while the PDG calculation is favored at the lowest and highest p_{T}.

Results from two event generators are also shown in Fig. 2. The black dashed line is a calculation from PYTHIA8, using the default settings. This model shows little variation with p_{T}, but is consistent with the data for $p_{\mathrm{T}} > 20$ GeV/c. Results from the EPOS4HQ event generator [59] are given for two configurations. The dashed orange curve shows the ratio where all b quarks are required to hadronize via fragmentation, which is largely consistent with the result from PYTHIA8, and does not match the data at low p_{T}. The other EPOS4HQ calculation, shown in the red dashed line ("EPOS4HQ + coal"), includes quark coalescence as an additional hadronization mechanism for b quarks. This model reproduces the shape of the data, but slightly overpredicts the magnitude of the $\sigma_{\Lambda_b^0}/\sigma_{B^0}$ ratio at intermediate p_{T}. This could indicate that quark coalescence plays a role in baryon formation at relatively low p_{T}, while high-p_{T} b hadrons are formed primarily through fragmentation in vacuum.

The p_{T}-integrated $\sigma_{\Lambda_b^0}/\sigma_{B^0}$ ratio is shown as a function of multiplicity in Fig. 3. Numerical values are given in the Supplemental Material [55]. The error bars represent the quadrature sum of the statistical and systematic uncertainties, while the global uncertainty of $^{+19\%}_{-16\%}$ due to the branching fractions is indicated in text. In the lowest multiplicity bins, this pp data approaches the baryon fraction measured in e^+e^- collisions at the Large Electron-Position collider (LEP) [61]. This is expected since b quarks in low-multiplicity events do not overlap with other particles and fragment in the vacuum, as in e^+e^- collisions. There is a distinct rise of the baryon fraction with multiplicity, which plateaus at ~0.5 for collisions that produce more than twice the average number of VELO tracks, though the data at the highest multiplicities have increasing uncertainties. This could indicate that coalescence emerges as an additional production mechanism for baryons at high multiplicity, where multiple quark wave functions overlap.

The $\sigma_{\Lambda_b^0}/\sigma_{B^0}$ ratio is shown in Fig. 4 as a function of p_{T} in different multiplicity bins. Numerical values are given in the Supplemental Material [55]. The left panel shows the data in the different bins of total track multiplicity, where the multiplicity intervals correspond to less than $\langle N_{\mathrm{tracks}}^{\mathrm{VELO}}\rangle_{\mathrm{NB}}$, between 1 and 2 times $\langle N_{\mathrm{tracks}}^{\mathrm{VELO}}\rangle_{\mathrm{NB}}$, and

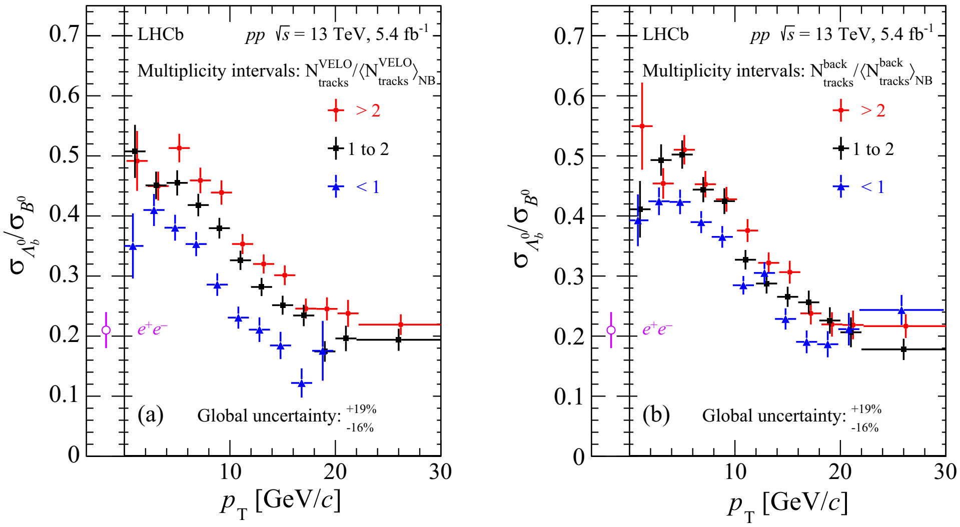

FIG. 4. Ratio of Λ_b^0 to B^0 cross sections as a function of p_{T}, in bins of (a) the total multiplicity measured in the VELO detector and (b) the backwards track multiplicity. The purple point shows the value measured in $e^+e^- \to Z^0 \to b\bar{b}$ reactions at LEP [61].

greater than twice $\langle N^{\mathrm{VELO}}_{\mathrm{tracks}}\rangle_{\mathrm{NB}}$. The right panel shows similar data, but uses $\langle N^{\mathrm{back}}_{\mathrm{tracks}}\rangle_{\mathrm{NB}}$ to define multiplicity. The error bars represent the quadrature sum of the statistical and systematic uncertainties, while the global uncertainty on all data points due to the uncertainties on the branching fractions is indicated in text. The purple point represents the LEP measurement of the ratio of the b-baryon fraction to b-meson fraction [61].

A significant multiplicity dependence can be observed using both multiplicity metrics, with higher multiplicity collisions displaying a larger Λ_b^0 fraction. The dependence is more pronounced when using the total number of VELO tracks (dominated by forward tracks), where there is clear ordering at intermediate p_{T}, however the backwards VELO tracks metric also shows a clear difference between the lowest and higher multiplicity bins. At low p_{T}, the ratio $\sigma_{\Lambda_b^0}/\sigma_{B^0}$ is significantly higher than the value measured in e^+e^- collisions, but as p_{T} increases the multiplicity dependence weakens and all data converges to the value from LEP. This is expected in quark coalescence scenarios, where low-p_{T} Λ_b^0 baryons can be produced when b quarks combine with two light quarks. However, at high-p_{T} Λ_b^0 baryons have limited overlap with the underlying event and are therefore produced by b-quark fragmentation in the vacuum.

In summary, these new measurements from LHCb show clear variations of the $\sigma_{\Lambda_b^0}/\sigma_{B^0}$ ratio with multiplicity and p_{T} in pp collisions at $\sqrt{s} = 13$ TeV. Production of the Λ_b^0 baryon is enhanced relative to the B^0 meson at high charged-particle multiplicity and relatively low p_{T}. The baryon fraction measured at LEP can be reached in pp collisions with very low multiplicity, and with b hadrons at high p_{T}, regardless of multiplicity. These observations show that b-quark hadronization is not universal between e^+e^- and pp collisions, and may indicate that quark coalescence plays an important role in forming hadrons at the LHC. These results are qualitatively consistent with the emergence of coalescence as an additional baryon production mechanism in high-density hadronic environments.

We express our gratitude to our colleagues in the CERN accelerator departments for the excellent performance of the LHC. We thank the technical and administrative staff at the LHCb institutes. We acknowledge support from CERN and from the national agencies: CAPES, CNPq, FAPERJ, and FINEP (Brazil); MOST and NSFC (China); CNRS/IN2P3 (France); BMBF, DFG and MPG (Germany); INFN (Italy); NWO (Netherlands); MNiSW and NCN (Poland); MCID/IFA (Romania); MICINN (Spain); SNSF and SER (Switzerland); NASU (Ukraine); STFC (United Kingdom); DOE NP and NSF (USA). We acknowledge the computing resources that are provided by CERN, IN2P3 (France), KIT, and DESY (Germany), INFN (Italy), SURF (Netherlands), PIC (Spain), GridPP (United Kingdom), CSCS (Switzerland), IFIN-HH (Romania), CBPF (Brazil), Polish WLCG (Poland), and NERSC (USA). We are indebted to the communities behind the multiple open-source software packages on which we depend. Individual groups or members have received support from ARC and ARDC (Australia); Key Research Program of Frontier Sciences of CAS, CAS PIFI, CAS CCEPP, Fundamental Research Funds for the Central Universities, and Sci. & Tech. Program of Guangzhou (China); Minciencias (Colombia); EPLANET, Marie Skłodowska-Curie Actions, ERC and NextGenerationEU (European Union); A*MIDEX, ANR, IPhU, and Labex P2IO, and Région Auvergne-Rhône-Alpes (France); AvH Foundation

(Germany); ICSC (Italy); GVA, XuntaGal, GENCAT, Inditex, InTalent and Prog. Atracción Talento, CM (Spain); SRC (Sweden); the Leverhulme Trust, the Royal Society, and UKRI (United Kingdom).

[1] K. G. Wilson, Confinement of quarks, Phys. Rev. D **10**, 2445 (1974).
[2] J. C. Collins, D. E. Soper, and G. F. Sterman, Factorization of hard processes in QCD, Adv. Ser. Dir. High Energy Phys. **5**, 1 (1989).
[3] B. Andersson, G. Gustafson, G. Ingelman, and T. Sjostrand, Parton fragmentation and string dynamics, Phys. Rep. **97**, 31 (1983).
[4] B. R. Webber, A QCD model for jet fragmentation including soft gluon interference, Nucl. Phys. **B238**, 492 (1984).
[5] R. D. Field and R. P. Feynman, A parametrization of the properties of quark jets, Nucl. Phys. **B136**, 1 (1978).
[6] D. P. Barber *et al.*, Discovery of three jet events and a test of quantum chromodynamics at PETRA energies, Phys. Rev. Lett. **43**, 830 (1979).
[7] W. Bartel *et al.* (JADE Collaboration), Experimental studies on multi-jet production in e^+e^- annihilation at PETRA energies, Z. Phys. C **33**, 23 (1986).
[8] A. H. Mueller, Jets at LEP and HERA, J. Phys. G **17**, 1443 (1991).
[9] F. Abe *et al.* (CDF Collaboration), Inclusive jet cross section in $\bar{p}p$ collisions at $\sqrt{s} = 1.8$ TeV, Phys. Rev. Lett. **77**, 438 (1996).
[10] V. M. Abazov *et al.* (D0 Collaboration), Measurement of the inclusive jet cross-section in $p\bar{p}$ collisions at $\sqrt{s} = 1.96$ TeV, Phys. Rev. Lett. **101**, 062001 (2008).
[11] A. Bhatti and D. Lincoln, Jet physics at the tevatron, Annu. Rev. Nucl. Part. Sci. **60**, 267 (2010).
[12] R. Kogler, B. Nachman, A. Schmidt, L. Asquith, E. Winkels *et al.*, Jet substructure at the Large Hadron Collider: Experimental review, Rev. Mod. Phys. **91**, 045003 (2019).
[13] M. Connors, C. Nattrass, R. Reed, and S. Salur, Jet measurements in heavy ion physics, Rev. Mod. Phys. **90**, 025005 (2018).
[14] B. A. Kniehl, G. Kramer, and B. Potter, Testing the universality of fragmentation functions, Nucl. Phys. **B597**, 337 (2001).
[15] A. Metz and A. Vossen, Parton fragmentation functions, Prog. Part. Nucl. Phys. **91**, 136 (2016).
[16] D. de Florian, R. Sassot, and M. Stratmann, Global analysis of fragmentation functions for pions and kaons and their uncertainties, Phys. Rev. D **75**, 114010 (2007).
[17] K. P. Das and R. C. Hwa, Quark-antiquark recombination in the fragmentation region, Phys. Lett. **68B**, 459 (1977); **73B**, 504(E) (1978).
[18] R. Vogt and S. J. Brodsky, QCD and intrinsic heavy quark predictions for leading charm and beauty hadroproduction, Nucl. Phys. **B438**, 261 (1995).
[19] E. Braaten, Y. Jia, and T. Mehen, The leading particle effect from heavy quark recombination, Phys. Rev. Lett. **89**, 122002 (2002).
[20] R. Rapp and E. V. Shuryak, D meson production from recombination in hadronic collisions, Phys. Rev. D **67**, 074036 (2003).
[21] M. He and R. Rapp, Hadronization and charm-hadron ratios in heavy-ion collisions, Phys. Rev. Lett. **124**, 042301 (2020).
[22] R. J. Fries, B. Muller, C. Nonaka, and S. A. Bass, Hadron production in heavy ion collisions: Fragmentation and recombination from a dense parton phase, Phys. Rev. C **68**, 044902 (2003).
[23] R. C. Hwa and C. B. Yang, Scaling behavior at high p_{T} and the p/π ratio, Phys. Rev. C **67**, 034902 (2003).
[24] R. J. Fries, B. Muller, C. Nonaka, and S. A. Bass, Hadronization in heavy ion collisions: Recombination and fragmentation of partons, Phys. Rev. Lett. **90**, 202303 (2003).
[25] V. Greco, C. M. Ko, and P. Levai, Parton coalescence and anti-proton/pion anomaly at RHIC, Phys. Rev. Lett. **90**, 202302 (2003).
[26] E. Norrbin and T. Sjostrand, Production and hadronization of heavy quarks, Eur. Phys. J. C **17**, 137 (2000).
[27] R. Aaij *et al.* (LHCb Collaboration), Measurement of the b-quark production cross-section in 7 and 13 TeV pp collisions, Phys. Rev. Lett. **118** (2017) 052002; **119**, 169901(E) (2017).
[28] R. Aaij *et al.* (LHCb Collaboration), Measurement of the $B^{\pm}$ production cross-section in $p\ p$ collisions at $\sqrt{s} = 7$ and 13 TeV, J. High Energy Phys. 12 (2017) 026.
[29] S. Acharya *et al.* (ALICE Collaboration), Measurement of beauty and charm production in pp collisions at $\sqrt{s} =$ 5.02 TeV via non-prompt and prompt D mesons, J. High Energy Phys. 05 (2021) 220.
[30] R. Aaij *et al.* (LHCb Collaboration), Measurement of b hadron production fractions in 7 TeV $p\ p$ collisions, Phys. Rev. D **85**, 032008 (2012).
[31] R. Aaij *et al.* (LHCb Collaboration), Measurement of b-hadron fractions in 13 TeV $p\ p$ collisions, Phys. Rev. D **100**, 031102(R) (2019).
[32] R. Aaij *et al.* (LHCb Collaboration), Observation of a $\Lambda_b^0 - \bar{\Lambda}_b^0$ production asymmetry in proton-proton collisions at $\sqrt{s} = 7$ and 8 TeV, J. High Energy Phys. 10 (2021) 060.
[33] R. Aaij *et al.* (LHCb Collaboration), Modification of b quark hadronization in high-multiplicity pp collisions at $\sqrt{s} = 13$ TeV, Phys. Rev. Lett. **131**, 061901 (2023).
[34] S. Acharya *et al.* (ALICE Collaboration), Charm-quark fragmentation fractions and production cross section at midrapidity in pp collisions at the LHC, Phys. Rev. D **105**, L011103 (2022).
[35] S. Acharya *et al.* (ALICE Collaboration), Observation of a multiplicity dependence in the p_T-differential charm baryon-to-meson ratios in proton–proton collisions at $\sqrt{s} = 13$ TeV, Phys. Lett. B **829**, 137065 (2022).
[36] A. A. Alves, Jr. *et al.* (LHCb Collaboration), The LHCb detector at the LHC, J. Instrum. **3**, S08005 (2008).
[37] R. Aaij *et al.* (LHCb Collaboration), LHCb detector performance, Int. J. Mod. Phys. A **30**, 1530022 (2015).
[38] R. Aaij *et al.*, Performance of the LHCb Vertex Locator, J. Instrum. **9**, P09007 (2014).
[39] P. d'Argent *et al.*, Improved performance of the LHCb outer tracker in LHC Run 2, J. Instrum. **12**, P11016 (2017).

[40] M. Adinolfi *et al.*, Performance of the LHCb RICH detector at the LHC, Eur. Phys. J. C **73**, 2431 (2013).
[41] A. A. Alves, Jr. *et al.*, Performance of the LHCb muon system, J. Instrum. **8**, P02022 (2013).
[42] T. Sjöstrand, S. Mrenna, and P. Skands, A brief introduction to PYTHIA8.1, Comput. Phys. Commun. **178**, 852 (2008).
[43] D. J. Lange, The EVTGEN particle decay simulation package, Nucl. Instrum. Methods Phys. Res., Sect. A **462**, 152 (2001).
[44] N. Davidson, T. Przedzinski, and Z. Was, PHOTOS interface in C++: Technical and physics documentation, Comput. Phys. Commun. **199**, 86 (2016).
[45] J. Allison *et al.* (Geant4 Collaboration), Geant4 developments and applications, IEEE Trans. Nucl. Sci. **53**, 270 (2006).
[46] M. Clemencic, G. Corti, S. Easo, C. R. Jones, S. Miglioranzi, M. Pappagallo, and P. Robbe, The LHCb simulation application, Gauss: Design, evolution and experience, J. Phys. Conf. Ser. **331**, 032023 (2011).
[47] M. Pivk and F. R. Le Diberder, SPlot: A statistical tool to unfold data distributions, Nucl. Instrum. Methods Phys. Res., Sect. A **555**, 356 (2005).
[48] P. A. Zyla *et al.* (Particle Data Group), Review of particle physics, Prog. Theor. Exp. Phys. **2020**, 083C01 (2020).
[49] T. Skwarnicki, A study of the radiative cascade transitions between the Upsilon-prime and Upsilon resonances, Ph.D. thesis, Institute of Nuclear Physics, Krakow, DESY-F31-86-02, 1986.
[50] S. Tolk, J. Albrecht, F. Dettori, and A. Pellegrino, Data driven trigger efficiency determination at LHCb, LHCb-PUB-2014-039, CERN, 2014, https://cds.cern.ch/record/1701134.
[51] R. Aaij *et al.* (LHCb Collaboration), Observation of $J/\psi p$ resonances consistent with pentaquark states in $\Lambda_b^0 \to J/\psi p K^-$ decays, Phys. Rev. Lett. **115**, 072001 (2015).
[52] R. Aaij *et al.* (LHCb Collaboration), Model-independent observation of exotic contributions to $B^0 \to J/\psi K^+ \pi^-$ decays, Phys. Rev. Lett. **122**, 152002 (2019).
[53] R. Aaij *et al.* (LHCb Collaboration), Observation of a narrow pentaquark state, $P_c(4312)^+$, and of two-peak structure of the $P_c(4450)^+$, Phys. Rev. Lett. **122**, 222001 (2019).
[54] L. Anderlini *et al.*, The PIDCALIB package, LHCb-PUB-2016-021, CERN, 2016, https://cds.cern.ch/record/2202412.
[55] See Supplemental Material at http://link.aps.org/supplemental/10.1103/PhysRevLett.132.081901 for numerical values of cross section ratios.
[56] R. Aaij *et al.* (LHCb Collaboration), Measurement of B meson production cross-sections in proton-proton collisions at $\sqrt{s} = 7$ TeV, J. High Energy Phys. 08 (2013) 117.
[57] R. Aaij *et al.* (LHCb Collaboration), Measurement of B^+, B^0 and Λ_b^0 production in p Pb collisions at $\sqrt{s_{\mathrm{NN}}} = 8.16$ TeV, Phys. Rev. D **99**, 052011 (2019).
[58] M. He and R. Rapp, Bottom hadrochemistry in high-energy hadronic collisions, Phys. Rev. Lett. **131**, 012301 (2023).
[59] J. Zhao, J. Aichelin, P. B. Gossiaux, and K. Werner, Heavy flavor as a probe of hot QCD matter produced in proton-proton collisions, arXiv:2310.08684.
[60] D. Ebert, R. N. Faustov, and V. O. Galkin, Spectroscopy and Regge trajectories of heavy baryons in the relativistic quark-diquark picture, Phys. Rev. D **84**, 014025 (2011).
[61] Y. Amhis *et al.* (Heavy Flavor Averaging Group), Averages of b-hadron, c-hadron, and τ-lepton properties as of 2018, Eur. Phys. J. C **81**, 226 (2021).

R. Aaij,[35] A. S. W. Abdelmotteleb,[54] C. Abellan Beteta,[48] F. Abudinén,[54] T. Ackernley,[58] B. Adeva,[44] M. Adinolfi,[52] P. Adlarson,[78] C. Agapopoulou,[46] C. A. Aidala,[79] Z. Ajaltouni,[11] S. Akar,[63] K. Akiba,[35] P. Albicocco,[25] J. Albrecht,[17] F. Alessio,[46] M. Alexander,[57] A. Alfonso Albero,[43] Z. Aliouche,[60] P. Alvarez Cartelle,[53] R. Amalric,[15] S. Amato,[3] J. L. Amey,[52] Y. Amhis,[13,46] L. An,[6] L. Anderlini,[24] M. Andersson,[48] A. Andreianov,[41] P. Andreola,[48] M. Andreotti,[23] D. Andreou,[66] A. A. Anelli,[28,b] D. Ao,[7] F. Archilli,[34,c] M. Argenton,[23] S. Arguedas Cuendis,[9] A. Artamonov,[41] M. Artuso,[66] E. Aslanides,[12] M. Atzeni,[62] B. Audurier,[14] D. Bacher,[61] I. Bachiller Perea,[10] S. Bachmann,[19] M. Bachmayer,[47] J. J. Back,[54] A. Bailly-reyre,[15] P. Baladron Rodriguez,[44] V. Balagura,[14] W. Baldini,[23] J. Baptista de Souza Leite,[2] M. Barbetti,[24,d] I. R. Barbosa,[67] R. J. Barlow,[60] S. Barsuk,[13] W. Barter,[56] M. Bartolini,[53] F. Baryshnikov,[41] J. M. Basels,[16] G. Bassi,[32,e] B. Batsukh,[5] A. Battig,[17] A. Bay,[47] A. Beck,[54] M. Becker,[17] F. Bedeschi,[32] I. B. Bediaga,[2] A. Beiter,[66] S. Belin,[44] V. Bellee,[48] K. Belous,[41] I. Belov,[26] I. Belyaev,[41] G. Benane,[12] G. Bencivenni,[25] E. Ben-Haim,[15] A. Berezhnoy,[41] J. L. M. Berkey,[65] R. Bernet,[48] S. Bernet Andres,[42] H. C. Bernstein,[66] C. Bertella,[60] A. Bertolin,[30] C. Betancourt,[48] F. Betti,[56] J. Bex,[53] Ia. Bezshyiko,[48] J. Bhom,[38] M. S. Bieker,[17] N. V. Biesuz,[23] P. Billoir,[15] A. Biolchini,[35] M. Birch,[59] F. C. R. Bishop,[10] A. Bitadze,[60] A. Bizzeti, M. P. Blago,[53] T. Blake,[54] F. Blanc,[47] J. E. Blank,[17] S. Blusk,[66] D. Bobulska,[57] V. Bocharnikov,[41] J. A. Boelhauve,[17] O. Boente Garcia,[14] T. Boettcher,[63] A. Bohare,[56] A. Boldyrev,[41] C. S. Bolognani,[76] R. Bolzonella,[23,f] N. Bondar,[41] F. Borgato,[30,46] S. Borghi,[60] M. Borsato,[28,b] J. T. Borsuk,[38] S. A. Bouchiba,[47] T. J. V. Bowcock,[58] A. Boyer,[46] C. Bozzi,[23] M. J. Bradley,[59] S. Braun,[64] A. Brea Rodriguez,[44] N. Breer,[17] J. Brodzicka,[38] A. Brossa Gonzalo,[44] J. Brown,[58] D. Brundu,[29] A. Buonaura,[48] L. Buonincontri,[30]

A. T. Burke,[60] C. Burr,[46] A. Bursche,[69] A. Butkevich,[41] J. S. Butter,[53] J. Buytaert,[46] W. Byczynski,[46] S. Cadeddu,[29] H. Cai,[71] R. Calabrese,[23,f] L. Calefice,[17] S. Cali,[25] M. Calvi,[28,b] M. Calvo Gomez,[42] J. Cambon Bouzas,[44] P. Campana,[25] D. H. Campora Perez,[76] A. F. Campoverde Quezada,[7] S. Capelli,[28,b] L. Capriotti,[23] R. Caravaca-Mora,[9] A. Carbone,[22,g] L. Carcedo Salgado,[44] R. Cardinale,[26,h] A. Cardini,[29] P. Carniti,[28,b] L. Carus,[19] A. Casais Vidal,[62] R. Caspary,[19] G. Casse,[58] J. Castro Godinez,[9] M. Cattaneo,[46] G. Cavallero,[23] V. Cavallini,[23,f] S. Celani,[47] J. Cerasoli,[12] D. Cervenkov,[61] S. Cesare,[27,i] A. J. Chadwick,[58] I. Chahrour,[79] M. Charles,[15] Ph. Charpentier,[46] C. A. Chavez Barajas,[58] M. Chefdeville,[10] C. Chen,[12] S. Chen,[5] A. Chernov,[38] S. Chernyshenko,[50] V. Chobanova,[44,j] S. Cholak,[47] M. Chrzaszcz,[38] A. Chubykin,[41] V. Chulikov,[41] P. Ciambrone,[25] M. F. Cicala,[54] X. Cid Vidal,[44] G. Ciezarek,[46] P. Cifra,[46] P. E. L. Clarke,[56] M. Clemencic,[46] H. V. Cliff,[53] J. Closier,[46] J. L. Cobbledick,[60] C. Cocha Toapaxi,[19] V. Coco,[46] J. Cogan,[12] E. Cogneras,[11] L. Cojocariu,[40] P. Collins,[46] T. Colombo,[46] A. Comerma-Montells,[43] L. Congedo,[21] A. Contu,[29] N. Cooke,[57] I. Corredoira,[44] A. Correia,[15] G. Corti,[46] J. J. Cottee Meldrum,[52] B. Couturier,[46] D. C. Craik,[48] M. Cruz Torres,[2,k] R. Currie,[56] C. L. Da Silva,[65] S. Dadabaev,[41] L. Dai,[68] X. Dai,[6] E. Dall'Occo,[17] J. Dalseno,[44] C. D'Ambrosio,[46] J. Daniel,[11] A. Danilina,[41] P. d'Argent,[21] A. Davidson,[54] J. E. Davies,[60] A. Davis,[60] O. De Aguiar Francisco,[60] C. De Angelis,[29,l] J. de Boer,[35] K. De Bruyn,[75] S. De Capua,[60] M. De Cian,[19,46] U. De Freitas Carneiro Da Graca,[2,m] E. De Lucia,[25] J. M. De Miranda,[2] L. De Paula,[3] M. De Serio,[21,n] D. De Simone,[48] P. De Simone,[25] F. De Vellis,[17] J. A. de Vries,[76] F. Debernardis,[21,n] D. Decamp,[10] V. Dedu,[12] L. Del Buono,[15] B. Delaney,[62] H.-P. Dembinski,[17] J. Deng,[8] V. Denysenko,[48] O. Deschamps,[11] F. Dettori,[29,l] B. Dey,[74] P. Di Nezza,[25] I. Diachkov,[41] S. Didenko,[41] S. Ding,[66] V. Dobishuk,[50] A. D. Docheva,[57] A. Dolmatov,[41] C. Dong,[4] A. M. Donohoe,[20] F. Dordei,[29] A. C. dos Reis,[2] L. Douglas,[57] A. G. Downes,[10] W. Duan,[69] P. Duda,[77] M. W. Dudek,[38] L. Dufour,[46] V. Duk,[31] P. Durante,[46] M. M. Duras,[77] J. M. Durham,[65] D. Dutta,[60] A. Dziurda,[38] A. Dzyuba,[41] S. Easo,[55,46] E. Eckstein,[73] U. Egede,[1] A. Egorychev,[41] V. Egorychev,[41] C. Eirea Orro,[44] S. Eisenhardt,[56] E. Ejopu,[60] S. Ek-In,[47] L. Eklund,[78] M. Elashri,[63] J. Ellbracht,[17] S. Ely,[59] A. Ene,[40] E. Epple,[63] S. Escher,[16] J. Eschle,[48] S. Esen,[48] T. Evans,[60] F. Fabiano,[29,46,l] L. N. Falcao,[2] Y. Fan,[7] B. Fang,[71,13] L. Fantini,[31,o] M. Faria,[47] K. Farmer,[56] D. Fazzini,[28,b] L. Felkowski,[77] M. Feng,[5,7] M. Feo,[46] M. Fernandez Gomez,[44] A. D. Fernez,[64] F. Ferrari,[22] F. Ferreira Rodrigues,[3] S. Ferreres Sole,[35] M. Ferrillo,[48] M. Ferro-Luzzi,[46] S. Filippov,[41] R. A. Fini,[21] M. Fiorini,[23,f] M. Firlej,[37] K. M. Fischer,[61] D. S. Fitzgerald,[79] C. Fitzpatrick,[60] T. Fiutowski,[37] F. Fleuret,[14] M. Fontana,[22] F. Fontanelli,[26,h] L. F. Foreman,[60] R. Forty,[46] D. Foulds-Holt,[53] M. Franco Sevilla,[64] M. Frank,[46] E. Franzoso,[23,f] G. Frau,[19] C. Frei,[46] D. A. Friday,[60] L. Frontini,[27,i] J. Fu,[7] Q. Fuehring,[17] Y. Fujii,[1] T. Fulghesu,[15] E. Gabriel,[35] G. Galati,[21,n] M. D. Galati,[35] A. Gallas Torreira,[44] D. Galli,[22,g] S. Gambetta,[56,46] M. Gandelman,[3] P. Gandini,[27] H. Gao,[7] R. Gao,[61] Y. Gao,[8] Y. Gao,[6] Y. Gao,[8] M. Garau,[29,l] L. M. Garcia Martin,[47] P. Garcia Moreno,[43] J. García Pardiñas,[46] B. Garcia Plana,[44] K. G. Garg,[8] L. Garrido,[43] C. Gaspar,[46] R. E. Geertsema,[35] L. L. Gerken,[17] E. Gersabeck,[60] M. Gersabeck,[60] T. Gershon,[54] Z. Ghorbanimoghaddam,[52] L. Giambastiani,[30] F. I. Giasemis,[15,p] V. Gibson,[53] H. K. Giemza,[39] A. L. Gilman,[61] M. Giovannetti,[25] A. Gioventù,[43] P. Gironella Gironell,[43] C. Giugliano,[23,f] M. A. Giza,[38] E. L. Gkougkousis,[59] F. C. Glaser,[13,19] V. V. Gligorov,[15] C. Göbel,[67] E. Golobardes,[42] D. Golubkov,[41] A. Golutvin,[59,41,46] A. Gomes,[2,a,q] S. Gomez Fernandez,[43] F. Goncalves Abrantes,[61] M. Goncerz,[38] G. Gong,[4] J. A. Gooding,[17] I. V. Gorelov,[41] C. Gotti,[28] J. P. Grabowski,[73] L. A. Granado Cardoso,[46] E. Graugés,[43] E. Graverini,[47] L. Grazette,[54] G. Graziani, A. T. Grecu,[40] L. M. Greeven,[35] N. A. Grieser,[63] L. Grillo,[57] S. Gromov,[41] C. Gu,[14] M. Guarise,[23] M. Guittiere,[13] V. Guliaeva,[41] P. A. Günther,[19] A.-K. Guseinov,[41] E. Gushchin,[41] Y. Guz,[6,41,46] T. Gys,[46] T. Hadavizadeh,[1] C. Hadjivasiliou,[64] G. Haefeli,[47] C. Haen,[46] J. Haimberger,[46] M. Hajheidari,[46] T. Halewood-leagas,[58] M. M. Halvorsen,[46] P. M. Hamilton,[64] J. Hammerich,[58] Q. Han,[8] X. Han,[19] S. Hansmann-Menzemer,[19] L. Hao,[7] N. Harnew,[61] T. Harrison,[58] M. Hartmann,[13] C. Hasse,[46] J. He,[7,r] K. Heijhoff,[35] F. Hemmer,[46] C. Henderson,[63] R. D. L. Henderson,[1,54] A. M. Hennequin,[46] K. Hennessy,[58] L. Henry,[47] J. Herd,[59] J. Heuel,[16] A. Hicheur,[3] D. Hill,[47] S. E. Hollitt,[17] J. Horswill,[60] R. Hou,[8] Y. Hou,[10] N. Howarth,[58] J. Hu,[19] J. Hu,[69] W. Hu,[6] X. Hu,[4] W. Huang,[7] W. Hulsbergen,[35] R. J. Hunter,[54] M. Hushchyn,[41] D. Hutchcroft,[58] M. Idzik,[37] D. Ilin,[41] P. Ilten,[63] A. Inglessi,[41] A. Iniukhin,[41] A. Ishteev,[41] K. Ivshin,[41] R. Jacobsson,[46] H. Jage,[16] S. J. Jaimes Elles,[45,72] S. Jakobsen,[46] E. Jans,[35] B. K. Jashal,[45] A. Jawahery,[64]

V. Jevtic,[17] E. Jiang,[64] X. Jiang,[5,7] Y. Jiang,[7] Y. J. Jiang,[6] M. John,[61] D. Johnson,[51] C. R. Jones,[53] T. P. Jones,[54] S. Joshi,[39] B. Jost,[46] N. Jurik,[46] I. Juszczak,[38] D. Kaminaris,[47] S. Kandybei,[49] Y. Kang,[4] M. Karacson,[46] D. Karpenkov,[41] M. Karpov,[41] A. M. Kauniskangas,[47] J. W. Kautz,[63] F. Keizer,[46] D. M. Keller,[66] M. Kenzie,[53] T. Ketel,[35] B. Khanji,[66] A. Kharisova,[41] S. Kholodenko,[32] G. Khreich,[13] T. Kirn,[16] V. S. Kirsebom,[47] O. Kitouni,[62] S. Klaver,[36] N. Kleijne,[32,e] K. Klimaszewski,[39] M. R. Kmiec,[39] S. Koliiev,[50] L. Kolk,[17] A. Konoplyannikov,[41] P. Kopciewicz,[37,46] P. Koppenburg,[35] M. Korolev,[41] I. Kostiuk,[35] O. Kot,[50] S. Kotriakhova, A. Kozachuk,[41] P. Kravchenko,[41] L. Kravchuk,[41] M. Kreps,[54] S. Kretzschmar,[16] P. Krokovny,[41] W. Krupa,[66] W. Krzemien,[39] J. Kubat,[19] S. Kubis,[77] W. Kucewicz,[38] M. Kucharczyk,[38] V. Kudryavtsev,[41] E. Kulikova,[41] A. Kupsc,[78] B. K. Kutsenko,[12] D. Lacarrere,[46] G. Lafferty,[60] A. Lai,[29] A. Lampis,[29] D. Lancierini,[48] C. Landesa Gomez,[44] J. J. Lane,[1] R. Lane,[52] C. Langenbruch,[19] J. Langer,[17] O. Lantwin,[41] T. Latham,[54] F. Lazzari,[32,s] C. Lazzeroni,[51] R. Le Gac,[12] S. H. Lee,[79] R. Lefèvre,[11] A. Leflat,[41] S. Legotin,[41] M. Lehuraux,[54] O. Leroy,[12] T. Lesiak,[38] B. Leverington,[19] A. Li,[4] H. Li,[69] K. Li,[8] L. Li,[60] P. Li,[46] P.-R. Li,[70] S. Li,[8] T. Li,[5] T. Li,[69] Y. Li,[8] Y. Li,[5] Z. Li,[66] Z. Lian,[4] X. Liang,[66] C. Lin,[7] T. Lin,[55] R. Lindner,[46] V. Lisovskyi,[47] R. Litvinov,[29,l] G. Liu,[69] H. Liu,[7] K. Liu,[70] Q. Liu,[7] S. Liu,[5,7] Y. Liu,[56] Y. Liu,[70] Y. L. Liu,[59] A. Lobo Salvia,[43] A. Loi,[29] J. Lomba Castro,[44] T. Long,[53] J. H. Lopes,[3] A. Lopez Huertas,[43] S. López Soliño,[44] G. H. Lovell,[53] C. Lucarelli,[24,d] D. Lucchesi,[30,t] S. Luchuk,[41] M. Lucio Martinez,[76] V. Lukashenko,[35,50] Y. Luo,[4] A. Lupato,[30] E. Luppi,[23,f] K. Lynch,[20] X.-R. Lyu,[7] G. M. Ma,[4] R. Ma,[7] S. Maccolini,[17] F. Machefert,[13] F. Maciuc,[40] I. Mackay,[61] L. R. Madhan Mohan,[53] M. M. Madurai,[51] A. Maevskiy,[41] D. Magdalinski,[35] D. Maisuzenko,[41] M. W. Majewski,[37] J. J. Malczewski,[38] S. Malde,[61] B. Malecki,[38,46] L. Malentacca,[46] A. Malinin,[41] T. Maltsev,[41] G. Manca,[29,l] G. Mancinelli,[12] C. Mancuso,[27,13,i] R. Manera Escalero,[43] D. Manuzzi,[22] D. Marangotto,[27,i] J. F. Marchand,[10] R. Marchevski,[47] U. Marconi,[22] S. Mariani,[46] C. Marin Benito,[43,46] J. Marks,[19] A. M. Marshall,[52] P. J. Marshall,[58] G. Martelli,[31,o] G. Martellotti,[33] L. Martinazzoli,[46] M. Martinelli,[28,b] D. Martinez Santos,[44] F. Martinez Vidal,[45] A. Massafferri,[2] M. Materok,[16] R. Matev,[46] A. Mathad,[48] V. Matiunin,[41] C. Matteuzzi,[66] K. R. Mattioli,[14] A. Mauri,[59] E. Maurice,[14] J. Mauricio,[43] P. Mayencourt,[47] M. Mazurek,[46] M. McCann,[59] L. Mcconnell,[20] T. H. McGrath,[60] N. T. McHugh,[57] A. McNab,[60] R. McNulty,[20] B. Meadows,[63] G. Meier,[17] D. Melnychuk,[39] M. Merk,[35,76] A. Merli,[27,i] L. Meyer Garcia,[3] D. Miao,[5,7] H. Miao,[7] M. Mikhasenko,[73,u] D. A. Milanes,[72] A. Minotti,[28,b] E. Minucci,[66] T. Miralles,[11] S. E. Mitchell,[56] B. Mitreska,[17] D. S. Mitzel,[17] A. Modak,[55] A. Mödden,[17] R. A. Mohammed,[61] R. D. Moise,[16] S. Mokhnenko,[41] T. Mombächer,[46] M. Monk,[54,1] I. A. Monroy,[72] S. Monteil,[11] A. Morcillo Gomez,[44] G. Morello,[25] M. J. Morello,[32,e] M. P. Morgenthaler,[19] J. Moron,[37] A. B. Morris,[46] A. G. Morris,[12] R. Mountain,[66] H. Mu,[4] Z. M. Mu,[6] E. Muhammad,[54] F. Muheim,[56] M. Mulder,[75] K. Müller,[48] F. Mũnoz-Rojas,[9] R. Murta,[59] P. Naik,[58] T. Nakada,[47] R. Nandakumar,[55] T. Nanut,[46] I. Nasteva,[3] M. Needham,[56] N. Neri,[27,i] S. Neubert,[73] N. Neufeld,[46] P. Neustroev,[41] R. Newcombe,[59] J. Nicolini,[17,13] D. Nicotra,[76] E. M. Niel,[47] N. Nikitin,[41] P. Nogga,[73] N. S. Nolte,[62] C. Normand,[10,29,l] J. Novoa Fernandez,[44] G. Nowak,[63] C. Nunez,[79] H. N. Nur,[57] A. Oblakowska-Mucha,[37] V. Obraztsov,[41] T. Oeser,[16] S. Okamura,[23,46,f] R. Oldeman,[29,l] F. Oliva,[56] M. Olocco,[17] C. J. G. Onderwater,[76] R. H. O'Neil,[56] J. M. Otalora Goicochea,[3] T. Ovsiannikova,[41] P. Owen,[48] A. Oyanguren,[45] O. Ozcelik,[56] K. O. Padeken,[73] B. Pagare,[54] P. R. Pais,[19] T. Pajero,[61] A. Palano,[21] M. Palutan,[25] G. Panshin,[41] L. Paolucci,[54] A. Papanestis,[55] M. Pappagallo,[21,n] L. L. Pappalardo,[23,f] C. Pappenheimer,[63] C. Parkes,[60] B. Passalacqua,[23,f] G. Passaleva,[24] D. Passaro,[32,e] A. Pastore,[21] M. Patel,[59] J. Patoc,[61] C. Patrignani,[22,g] C. J. Pawley,[76] A. Pellegrino,[35] M. Pepe Altarelli,[25] S. Perazzini,[22] D. Pereima,[41] A. Pereiro Castro,[44] P. Perret,[11] A. Perro,[46] K. Petridis,[52] A. Petrolini,[26,h] S. Petrucci,[56] H. Pham,[66] L. Pica,[32,e] M. Piccini,[31] B. Pietrzyk,[10] G. Pietrzyk,[13] D. Pinci,[33] F. Pisani,[46] M. Pizzichemi,[28,b] V. Placinta,[40] M. Plo Casasus,[44] F. Polci,[15,46] M. Poli Lener,[25] A. Poluektov,[12] N. Polukhina,[41] I. Polyakov,[46] E. Polycarpo,[3] S. Ponce,[46] D. Popov,[7] S. Poslavskii,[41] K. Prasanth,[38] L. Promberger,[19] C. Prouve,[44] V. Pugatch,[50] V. Puill,[13] G. Punzi,[32,s] H. R. Qi,[4] W. Qian,[7] N. Qin,[4] S. Qu,[4] R. Quagliani,[47] R. I. Rabadan Trejo,[54] B. Rachwal,[37] J. H. Rademacker,[52] M. Rama,[32] M. Ramírez García,[79] M. Ramos Pernas,[54] M. S. Rangel,[3] F. Ratnikov,[41] G. Raven,[36] M. Rebollo De Miguel,[45] F. Redi,[46] J. Reich,[52] F. Reiss,[60] Z. Ren,[7] P. K. Resmi,[61] R. Ribatti,[32,e] G. R. Ricart,[14,80] D. Riccardi,[32,e] S. Ricciardi,[55] K. Richardson,[62] M. Richardson-Slipper,[56] K. Rinnert,[58] P. Robbe,[13] G. Robertson,[57] E. Rodrigues,[58,46]

E. Rodriguez Fernandez,[44] J. A. Rodriguez Lopez,[72] E. Rodriguez Rodriguez,[44] A. Rogovskiy,[55] D. L. Rolf,[46] A. Rollings,[61] P. Roloff,[46] V. Romanovskiy,[41] M. Romero Lamas,[44] A. Romero Vidal,[44] G. Romolini,[23] F. Ronchetti,[47] M. Rotondo,[25] S. R. Roy,[19] M. S. Rudolph,[66] T. Ruf,[46] M. Ruiz Diaz,[19] R. A. Ruiz Fernandez,[44] J. Ruiz Vidal,[78,v] A. Ryzhikov,[41] J. Ryzka,[37] J. J. Saborido Silva,[44] R. Sadek,[14] N. Sagidova,[41] N. Sahoo,[51] B. Saitta,[29,l] M. Salomoni,[28,b] C. Sanchez Gras,[35] I. Sanderswood,[45] R. Santacesaria,[33] C. Santamarina Rios,[44] M. Santimaria,[25] L. Santoro,[2] E. Santovetti,[34] A. Saputi,[23,46] D. Saranin,[41] G. Sarpis,[56] M. Sarpis,[73] A. Sarti,[33] C. Satriano,[33,w] A. Satta,[34] M. Saur,[6] D. Savrina,[41] H. Sazak,[11] L. G. Scantlebury Smead,[61] A. Scarabotto,[15] S. Schael,[16] S. Scherl,[58] A. M. Schertz,[74] M. Schiller,[57] H. Schindler,[46] M. Schmelling,[18] B. Schmidt,[46] S. Schmitt,[16] H. Schmitz,[73] O. Schneider,[47] A. Schopper,[46] N. Schulte,[17] S. Schulte,[47] M. H. Schune,[13] R. Schwemmer,[46] G. Schwering,[16] B. Sciascia,[25] A. Sciuccati,[46] S. Sellam,[44] A. Semennikov,[41] M. Senghi Soares,[36] A. Sergi,[26,h] N. Serra,[48,46] L. Sestini,[30] A. Seuthe,[17] Y. Shang,[6] D. M. Shangase,[79] M. Shapkin,[41] I. Shchemerov,[41] L. Shchutska,[47] T. Shears,[58] L. Shekhtman,[41] Z. Shen,[6] S. Sheng,[5,7] V. Shevchenko,[41] B. Shi,[7] E. B. Shields,[28,b] Y. Shimizu,[13] E. Shmanin,[41] R. Shorkin,[41] J. D. Shupperd,[66] R. Silva Coutinho,[66] G. Simi,[30] S. Simone,[21,n] N. Skidmore,[60] R. Skuza,[19] T. Skwarnicki,[66] M. W. Slater,[51] J. C. Smallwood,[61] E. Smith,[62] K. Smith,[65] M. Smith,[59] A. Snoch,[35] L. Soares Lavra,[56] M. D. Sokoloff,[63] F. J. P. Soler,[57] A. Solomin,[41,52] A. Solovev,[41] I. Solovyev,[41] R. Song,[1] Y. Song,[47] Y. Song,[4] Y. S. Song,[6] F. L. Souza De Almeida,[66] B. Souza De Paula,[3] E. Spadaro Norella,[27,i] E. Spedicato,[22] J. G. Speer,[17] E. Spiridenkov,[41] P. Spradlin,[57] V. Sriskaran,[46] F. Stagni,[46] M. Stahl,[46] S. Stahl,[46] S. Stanislaus,[61] E. N. Stein,[46] O. Steinkamp,[48] O. Stenyakin,[41] H. Stevens,[17] D. Strekalina,[41] Y. Su,[7] F. Suljik,[61] J. Sun,[29] L. Sun,[71] Y. Sun,[64] P. N. Swallow,[51] K. Swientek,[37] F. Swystun,[54] A. Szabelski,[39] T. Szumlak,[37] M. Szymanski,[46] Y. Tan,[4] S. Taneja,[60] M. D. Tat,[61] A. Terentev,[48] F. Terzuoli,[32,x] F. Teubert,[46] E. Thomas,[46] D. J. D. Thompson,[51] H. Tilquin,[59] V. Tisserand,[11] S. T'Jampens,[10] M. Tobin,[5] L. Tomassetti,[23,f] G. Tonani,[27,i] X. Tong,[6] D. Torres Machado,[2] L. Toscano,[17] D. Y. Tou,[4] C. Trippl,[42] G. Tuci,[19] N. Tuning,[35] L. H. Uecker,[19] A. Ukleja,[37] D. J. Unverzagt,[19] E. Ursov,[41] A. Usachov,[36] A. Ustyuzhanin,[41] U. Uwer,[19] V. Vagnoni,[22] A. Valassi,[46] G. Valenti,[22] N. Valls Canudas,[42] H. Van Hecke,[65] E. van Herwijnen,[59] C. B. Van Hulse,[44,y] R. Van Laak,[47] M. van Veghel,[35] R. Vazquez Gomez,[43] P. Vazquez Regueiro,[44] C. Vázquez Sierra,[44] S. Vecchi,[23] J. J. Velthuis,[52] M. Veltri,[24,z] A. Venkateswaran,[47] M. Vesterinen,[54] D. Vieira,[63] M. Vieites Diaz,[46] X. Vilasis-Cardona,[42] E. Vilella Figueras,[58] A. Villa,[22] P. Vincent,[15] F. C. Volle,[13] D. vom Bruch,[12] V. Vorobyev,[41] N. Voropaev,[41] K. Vos,[76] G. Vouters,[10] C. Vrahas,[56] J. Walsh,[32] E. J. Walton,[1] G. Wan,[6] C. Wang,[19] G. Wang,[8] J. Wang,[6] J. Wang,[5] J. Wang,[4] J. Wang,[71] M. Wang,[27] N. W. Wang,[7] R. Wang,[52] X. Wang,[69] X. W. Wang,[59] Y. Wang,[8] Z. Wang,[13] Z. Wang,[4] Z. Wang,[7] J. A. Ward,[54,1] N. K. Watson,[51] D. Websdale,[59] Y. Wei,[6] B. D. C. Westhenry,[52] D. J. White,[60] M. Whitehead,[57] A. R. Wiederhold,[54] D. Wiedner,[17] G. Wilkinson,[61] M. K. Wilkinson,[63] M. Williams,[62] M. R. J. Williams,[56] R. Williams,[53] F. F. Wilson,[55] W. Wislicki,[39] M. Witek,[38] L. Witola,[19] C. P. Wong,[65] G. Wormser,[13] S. A. Wotton,[53] H. Wu,[66] J. Wu,[8] Y. Wu,[6] K. Wyllie,[46] S. Xian,[69] Z. Xiang,[5] Y. Xie,[8] A. Xu,[32] J. Xu,[7] L. Xu,[4] L. Xu,[4] M. Xu,[54] Z. Xu,[11] Z. Xu,[7] Z. Xu,[5] D. Yang,[4] S. Yang,[7] X. Yang,[6] Y. Yang,[26,h] Z. Yang,[6] Z. Yang,[64] V. Yeroshenko,[13] H. Yeung,[60] H. Yin,[8] C. Y. Yu,[6] J. Yu,[68] X. Yuan,[5] E. Zaffaroni,[47] M. Zavertyaev,[18] M. Zdybal,[38] M. Zeng,[4] C. Zhang,[6] D. Zhang,[8] J. Zhang,[7] L. Zhang,[4] S. Zhang,[68] S. Zhang,[6] Y. Zhang,[6] Y. Zhang,[61] Y. Z. Zhang,[4] Y. Zhao,[19] A. Zharkova,[41] A. Zhelezov,[19] X. Z. Zheng,[4] Y. Zheng,[7] T. Zhou,[6] X. Zhou,[8] Y. Zhou,[7] V. Zhovkovska,[54] L. Z. Zhu,[7] X. Zhu,[4] X. Zhu,[8] Z. Zhu,[7] V. Zhukov,[16,41] J. Zhuo,[45] Q. Zou,[5,7] D. Zuliani,[30] and G. Zunica[60]

(LHCb Collaboration)

[1]*School of Physics and Astronomy, Monash University, Melbourne, Australia*
[2]*Centro Brasileiro de Pesquisas Físicas (CBPF), Rio de Janeiro, Brazil*
[3]*Universidade Federal do Rio de Janeiro (UFRJ), Rio de Janeiro, Brazil*
[4]*Center for High Energy Physics, Tsinghua University, Beijing, China*
[5]*Institute Of High Energy Physics (IHEP), Beijing, China*
[6]*School of Physics State Key Laboratory of Nuclear Physics and Technology, Peking University, Beijing, China*

[7]*University of Chinese Academy of Sciences, Beijing, China*
[8]*Institute of Particle Physics, Central China Normal University, Wuhan, Hubei, China*
[9]*Consejo Nacional de Rectores (CONARE), San Jose, Costa Rica*
[10]*Université Savoie Mont Blanc, CNRS, IN2P3-LAPP, Annecy, France*
[11]*Université Clermont Auvergne, CNRS/IN2P3, LPC, Clermont-Ferrand, France*
[12]*Aix Marseille Univ, CNRS/IN2P3, CPPM, Marseille, France*
[13]*Université Paris-Saclay, CNRS/IN2P3, IJCLab, Orsay, France*
[14]*Laboratoire Leprince-Ringuet, CNRS/IN2P3, Ecole Polytechnique, Institut Polytechnique de Paris, Palaiseau, France*
[15]*LPNHE, Sorbonne Université, Paris Diderot Sorbonne Paris Cité, CNRS/IN2P3, Paris, France*
[16]*I. Physikalisches Institut, RWTH Aachen University, Aachen, Germany*
[17]*Fakultät Physik, Technische Universität Dortmund, Dortmund, Germany*
[18]*Max-Planck-Institut für Kernphysik (MPIK), Heidelberg, Germany*
[19]*Physikalisches Institut, Ruprecht-Karls-Universität Heidelberg, Heidelberg, Germany*
[20]*School of Physics, University College Dublin, Dublin, Ireland*
[21]*INFN Sezione di Bari, Bari, Italy*
[22]*INFN Sezione di Bologna, Bologna, Italy*
[23]*INFN Sezione di Ferrara, Ferrara, Italy*
[24]*INFN Sezione di Firenze, Firenze, Italy*
[25]*INFN Laboratori Nazionali di Frascati, Frascati, Italy*
[26]*INFN Sezione di Genova, Genova, Italy*
[27]*INFN Sezione di Milano, Milano, Italy*
[28]*INFN Sezione di Milano-Bicocca, Milano, Italy*
[29]*INFN Sezione di Cagliari, Monserrato, Italy*
[30]*Università degli Studi di Padova, Università e INFN, Padova, Padova, Italy*
[31]*INFN Sezione di Perugia, Perugia, Italy*
[32]*INFN Sezione di Pisa, Pisa, Italy*
[33]*INFN Sezione di Roma La Sapienza, Roma, Italy*
[34]*INFN Sezione di Roma Tor Vergata, Roma, Italy*
[35]*Nikhef National Institute for Subatomic Physics, Amsterdam, Netherlands*
[36]*Nikhef National Institute for Subatomic Physics and VU University Amsterdam, Amsterdam, Netherlands*
[37]*AGH - University of Science and Technology, Faculty of Physics and Applied Computer Science, Kraków, Poland*
[38]*Henryk Niewodniczanski Institute of Nuclear Physics Polish Academy of Sciences, Kraków, Poland*
[39]*National Center for Nuclear Research (NCBJ), Warsaw, Poland*
[40]*Horia Hulubei National Institute of Physics and Nuclear Engineering, Bucharest-Magurele, Romania*
[41]*Affiliated with an institute covered by a cooperation agreement with CERN*
[42]*DS4DS, La Salle, Universitat Ramon Llull, Barcelona, Spain*
[43]*ICCUB, Universitat de Barcelona, Barcelona, Spain*
[44]*Instituto Galego de Física de Altas Enerxías (IGFAE), Universidade de Santiago de Compostela, Santiago de Compostela, Spain*
[45]*Instituto de Fisica Corpuscular, Centro Mixto Universidad de Valencia - CSIC, Valencia, Spain*
[46]*European Organization for Nuclear Research (CERN), Geneva, Switzerland*
[47]*Institute of Physics, Ecole Polytechnique Fédérale de Lausanne (EPFL), Lausanne, Switzerland*
[48]*Physik-Institut, Universität Zürich, Zürich, Switzerland*
[49]*NSC Kharkiv Institute of Physics and Technology (NSC KIPT), Kharkiv, Ukraine*
[50]*Institute for Nuclear Research of the National Academy of Sciences (KINR), Kyiv, Ukraine*
[51]*University of Birmingham, Birmingham, United Kingdom*
[52]*H.H. Wills Physics Laboratory, University of Bristol, Bristol, United Kingdom*
[53]*Cavendish Laboratory, University of Cambridge, Cambridge, United Kingdom*
[54]*Department of Physics, University of Warwick, Coventry, United Kingdom*
[55]*STFC Rutherford Appleton Laboratory, Didcot, United Kingdom*
[56]*School of Physics and Astronomy, University of Edinburgh, Edinburgh, United Kingdom*
[57]*School of Physics and Astronomy, University of Glasgow, Glasgow, United Kingdom*
[58]*Oliver Lodge Laboratory, University of Liverpool, Liverpool, United Kingdom*
[59]*Imperial College London, London, United Kingdom*
[60]*Department of Physics and Astronomy, University of Manchester, Manchester, United Kingdom*
[61]*Department of Physics, University of Oxford, Oxford, United Kingdom*
[62]*Massachusetts Institute of Technology, Cambridge, Massachusetts, USA*
[63]*University of Cincinnati, Cincinnati, Ohio, USA*
[64]*University of Maryland, College Park, Maryland, USA*
[65]*Los Alamos National Laboratory (LANL), Los Alamos, New Mexico, USA*

[66]*Syracuse University, Syracuse, New York, USA*
[67]*Pontifícia Universidade Católica do Rio de Janeiro (PUC-Rio), Rio de Janeiro, Brazil*
(associated with Universidade Federal do Rio de Janeiro (UFRJ), Rio de Janeiro, Brazil)
[68]*School of Physics and Electronics, Hunan University, Changsha City, China*
(associated with Institute of Particle Physics, Central China Normal University, Wuhan, Hubei, China)
[69]*Guangdong Provincial Key Laboratory of Nuclear Science, Guangdong-Hong Kong Joint Laboratory of Quantum Matter, Institute of Quantum Matter, South China Normal University, Guangzhou, China*
(associated with Center for High Energy Physics, Tsinghua University, Beijing, China)
[70]*Lanzhou University, Lanzhou, China (associated with Institute Of High Energy Physics (IHEP), Beijing, China)*
[71]*School of Physics and Technology, Wuhan University, Wuhan, China*
(associated with Center for High Energy Physics, Tsinghua University, Beijing, China)
[72]*Departamento de Fisica, Universidad Nacional de Colombia, Bogota, Colombia*
(associated with LPNHE, Sorbonne Université, Paris Diderot Sorbonne Paris Cité, CNRS/IN2P3, Paris, France)
[73]*Universität Bonn - Helmholtz-Institut für Strahlen und Kernphysik, Bonn, Germany*
(associated with Physikalisches Institut, Ruprecht-Karls-Universität Heidelberg, Heidelberg, Germany)
[74]*Eotvos Lorand University, Budapest, Hungary*
(associated with European Organization for Nuclear Research (CERN), Geneva, Switzerland)
[75]*Van Swinderen Institute, University of Groningen, Groningen, Netherlands*
(associated with Nikhef National Institute for Subatomic Physics, Amsterdam, Netherlands)
[76]*Universiteit Maastricht, Maastricht, Netherlands*
(associated with Nikhef National Institute for Subatomic Physics, Amsterdam, Netherlands)
[77]*Tadeusz Kosciuszko Cracow University of Technology, Cracow, Poland*
(associated with Henryk Niewodniczanski Institute of Nuclear Physics Polish Academy of Sciences, Kraków, Poland)
[78]*Department of Physics and Astronomy, Uppsala University, Uppsala, Sweden*
(associated with School of Physics and Astronomy, University of Glasgow, Glasgow, United Kingdom)
[79]*University of Michigan, Ann Arbor, Michigan, USA*
(associated with Syracuse University, Syracuse, New York, USA)
[80]*Departement de Physique Nucleaire (SPhN), Gif-Sur-Yvette, France*

[a]Deceased.
[b]Also at Università di Milano Bicocca, Milano, Italy.
[c]Also at Università di Roma Tor Vergata, Roma, Italy.
[d]Also at Università di Firenze, Firenze, Italy.
[e]Also at Scuola Normale Superiore, Pisa, Italy.
[f]Also at Università di Ferrara, Ferrara, Italy.
[g]Also at Università di Bologna, Bologna, Italy.
[h]Also at Università di Genova, Genova, Italy.
[i]Also at Università degli Studi di Milano, Milano, Italy.
[j]Also at Universidade da Coruña, Coruña, Spain.
[k]Also at Universidad Nacional Autónoma de Honduras, Tegucigalpa, Honduras.
[l]Also at Università di Cagliari, Cagliari, Italy.
[m]Also at Centro Federal de Educacão Tecnológica Celso Suckow da Fonseca, Rio De Janeiro, Brazil.
[n]Also at Università di Bari, Bari, Italy.
[o]Also at Università di Perugia, Perugia, Italy.
[p]Also at LIP6, Sorbonne Universite, Paris, France.
[q]Also at Universidade de Brasília, Brasília, Brazil.
[r]Also at Hangzhou Institute for Advanced Study, UCAS, Hangzhou, China.
[s]Also at Università di Pisa, Pisa, Italy.
[t]Also at Università di Padova, Padova, Italy.
[u]Also at Excellence Cluster ORIGINS, Munich, Germany.
[v]Also at Department of Physics/Division of Particle Physics, Lund, Sweden.
[w]Also at Università della Basilicata, Potenza, Italy.
[x]Also at Università di Siena, Siena, Italy.
[y]Also at Universidad de Alcalá, Alcalá de Henares, Spain.
[z]Also at Università di Urbino, Urbino, Italy.